

See discussions, stats, and author profiles for this publication at: <https://www.researchgate.net/publication/51856432>

Existence of a New Emitting Singlet State of Proflavine: Femtosecond Dynamics of the Excited State Processes and Quantum Chemical Studies in Different Solvents

ARTICLE *in* THE JOURNAL OF PHYSICAL CHEMISTRY A · DECEMBER 2011

Impact Factor: 2.69 · DOI: 10.1021/jp207495r · Source: PubMed

CITATIONS

7

READS

35

4 AUTHORS, INCLUDING:



Karuppannan Senthilkumar

National University of Singapore

14 PUBLICATIONS 58 CITATIONS

SEE PROFILE



Selvaraju Chellappan

University of Madras

5 PUBLICATIONS 88 CITATIONS

SEE PROFILE



E. J. Padma Malar

University of Madras

62 PUBLICATIONS 538 CITATIONS

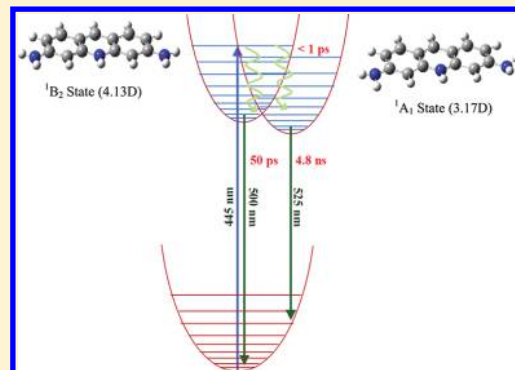
SEE PROFILE

Existence of a New Emitting Singlet State of Proflavine: Femtosecond Dynamics of the Excited State Processes and Quantum Chemical Studies in Different Solvents

Karuppannan Senthil Kumar, Chellappan Selvaraju, Ezekiel Joy Padma Malar, and Paramasivam Natarajan*

National Centre for Ultrafast Processes, Taramani Campus, University of Madras, Chennai 600 113, India

ABSTRACT: Proflavine (3,6-diaminoacridine) shows fluorescence emission with lifetime, 4.6 ± 0.2 ns, in all the solvents irrespective of the solvent polarity. To understand this unusual photophysical property, investigations were carried out using steady state and time-resolved fluorescence spectroscopy in the pico- and femtosecond time domain. Molecular geometries in the ground and low-lying excited states of proflavine were examined by complete structural optimization using ab initio quantum chemical computations at HF/6-311++G** and CIS/6-311++G** levels. Time dependent density functional theory (TDDFT) calculations were performed to study the excitation energies in the low-lying excited states. The steady state absorption and emission spectral details of proflavine are found to be influenced by solvents. The femtosecond fluorescence decay of the proflavine in all the solvents follows triexponential function with two ultrafast decay components (τ_1 and τ_2) in addition to the nanosecond component. The ultrafast decay component, τ_1 , is attributed to the solvation dynamics of the particular solvent used. The second ultrafast decay component, τ_2 , is found to vary from 50 to 215 ps depending upon the solvent. The amplitudes of the ultrafast decay components vary with the wavelength and show time dependent spectral shift in the emission maximum. The observation is interpreted that the time dependent spectral shift is not only due to solvation dynamics but also due to the existence of more than one emitting state of proflavine in the solvent used. Time resolved area normalized emission spectral (TRANES) analysis shows an isoemissive point, indicating the presence of two emitting states in homogeneous solution. Detailed femtosecond fluorescence decay analysis allows us to isolate the two independent emitting components of the close lying singlet states. The CIS and TDDFT calculations also support the existence of the close lying emitting states. The near constant lifetime observed for proflavine in different solvents is suggested to be due to the similar dipole moments of the ground and the evolved emitting singlet state of the dye from the Franck–Condon excited state.



1. INTRODUCTION

Proflavine (3,6-diaminoacridine), an acridine class of the dye, is known to be important for potential application in many areas of photobiology and in solar energy conversion.^{1–6} Proflavine has been shown to act as a sensitizer in the light induced hydrogen evolution from water.³ Understanding the detailed photophysics of the system is of importance because the excited state is showing photoredox behavior. Photophysics and the photochemistry of proflavine in aqueous and in micellar solution⁷ at different pHs have been studied extensively. The photophysical behavior of the dye covalently linked with polymer electrolytes has been investigated.⁸ Proflavine encapsulated in amine functionalized MCM-41 silicate host shows excited state proton transfer processes⁹ and the excited state proton transfer process from the host to the excited proflavine molecule loaded within a silane modified MCM-41 has also been reported.¹⁰ Mertz and co-workers¹¹ reported the static microscopic dielectric response of several dipolar solvents to charge redistribution in proflavine molecule. The macroscopic behavior and the relationship regarding the anomaly and fluctuating structures formed by solvents near the hydrophobic surface of the probe has also been

discussed. Proflavine, an intercalating dye, has been used to probe the dynamics of DNA.^{12–15} Studies on the interaction between proflavine and nucleic acid show spontaneous complex formation, and the interactions involve hydrogen bonding and electrostatic interaction between the dye and DNA. The studies on the femtosecond dynamics of the excited states of molecules are important to understand the interaction of the dye on optical excitation in the biological systems in microscopic level.

Elucidation of ultrafast excited state dynamics is also important for the understanding of the excited state properties of organic dyes and metal complexes in functional materials. A variety of fundamental phenomena including energy, electron transfer, and structural changes in the excited states are known to be important in the functional materials such as dye incorporated nanomaterials. The experimental measurements of the time-resolved Stokes shift in the emission spectra of the electronic excited states provide detailed information on the relaxation

Received: August 5, 2011

Revised: December 3, 2011

Published: December 06, 2011

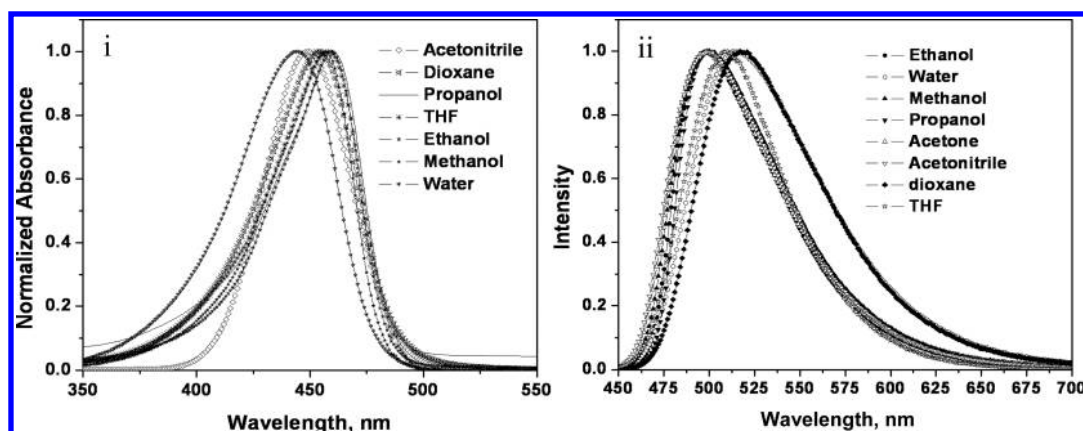


Figure 1. (i) Electronic absorption and (ii) emission spectra of proflavine in different solvents.

Table 1. Photophysical Characteristics of Proflavine in Various Solvents of Different Polarity (Excitation at 420 nm)

solvent	λ_{abs} , nm	λ_{em} , nm	Stokes shift, cm^{-1}	ϕ_f	τ , ns	dielectric constant
1, 4-dioxane	454	518	2721	0.38	4.53	2.22
THF	457	513	2388	0.52	4.57	7.52
acetone	455	497	1857	0.30	4.81	21.01
acetonitrile	451	496	2011	0.44	4.85	36.64
DMF	412	501	4311	0.50	4.80	38.3
1-propanol	460	499	1699	0.57	4.42	20.80
ethanol	459	497	1665	0.51	4.60	25.30
methanol	457	499	1841	0.40	4.80	33.00
water	444	513	3029	0.35	4.60	80.10

dynamics of molecules in solution and in supramolecular systems.^{16–18} Ultrafast fluorescence up-conversion techniques for measuring the emission decay processes with femtosecond time resolution are useful for determining the ultrafast evolution path of the excited states and related decay processes. Solvation dynamics and multistate emissions using femtosecond fluorescence up-conversion and the influence of the solvent have been reported earlier.^{19–21} At present, interest in the study of femtosecond dynamics of several organic dyes is growing rapidly.^{22–25} Recent progress in ultrafast spectroscopy provides new tools to investigate the very fast events occurring after photon absorption in homogeneous solution as well as with the dye encapsulated in to the nanoporous silicate hosts. The study of ultrafast spectroscopy of the organic dyes in solution as well as in solid hosts is useful to understand processes in dye sensitized solar cells.^{26–29} In the present work, we have studied in detail the photophysics of proflavine in solvents of different polarity using femtosecond fluorescence spectroscopy.

2. MATERIALS AND METHODS

2.1. Experimental Details. Proflavine obtained from Fluka was used after recrystallizing in ethanol. The solvents (HPLC grade) obtained from Qualigens were used as supplied. UV–visible absorption spectra of the samples were recorded in an Agilent 8453 spectrophotometer. Steady state fluorescence measurements of the dye in different solvents were carried out using

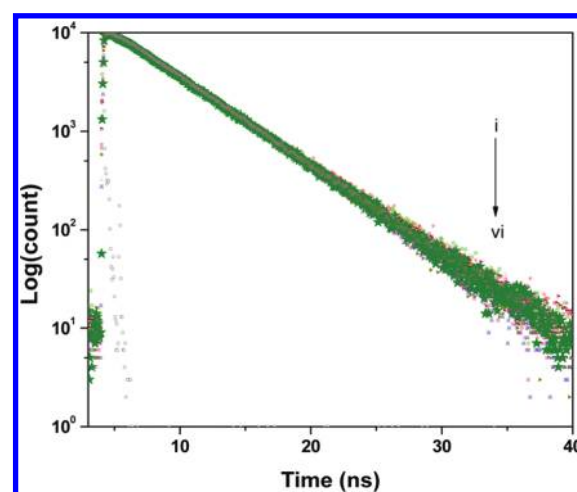


Figure 2. Fluorescence decay of proflavine in (i) 1, 4-dioxane, (ii) THF, (iii) acetone, (iv) acetonitrile, (v) 1-propanol, and (vi) water (excitation at 420 nm, decay monitored at 490 and 600 nm).

Jobin Yvon Fluoromax-4 spectrophotometer. Fluorescence quantum yields of proflavine in different solvents were measured using coumarin 153 as a reference with Φ_f for coumarin as 0.38 in ethanol.³⁰ Time resolved fluorescence measurements were carried out by time correlated single photon counting techniques exciting the sample at 420 nm laser. Data analysis was carried out by the software provided by IBH (DAS-6), which is based on deconvolution techniques using nonlinear least-squares method and the quality of the fit is ascertained with the value of $\chi^2 < 1.2$ and weighted residuals.

Femtosecond fluorescence decay was recorded using the fluorescence up-conversion technique. In the femtosecond up-conversion setup (FOG 100, CDP) the sample was excited using the second harmonic beam (420 nm, 200 fs) of a mode locked Ti-sapphire laser (Tsunami, Spectra Physics) pumped by DPPS (Millennia, Spectra Physics). The fundamental beam was frequency doubled using a nonlinear crystal (1 mm BBO, $\theta = 25^\circ$, $\phi = 90^\circ$). The sample was placed in a 1 mm thick rotating cell, and the fluorescence emission collected from the sample was up-converted in a nonlinear crystal (0.5 mm BBO, $\theta = 38^\circ$, $\phi = 90^\circ$) using a gate pulse of the fundamental beam. The up-converted light beam was dispersed through a monochromator and detected using the photon counting technique. The cross-correlation of

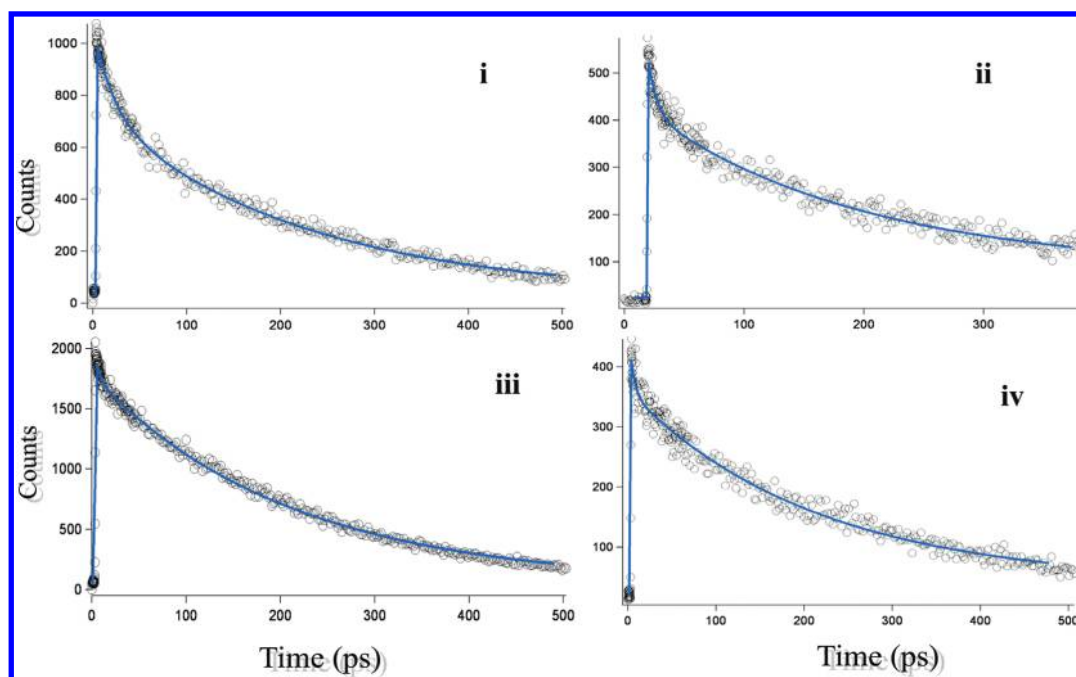


Figure 3. Femtosecond fluorescence decay of proflavine in (i) acetonitrile, (ii) ethanol, (iii) water, and (iv) 1,4-dioxane.

Table 2. Time Constants (τ) and Relative Amplitudes (A) of Functions Used in Fitting the Femtosecond Emission Transients of Proflavine in Different Solvents (Excitation at 420 nm and Decay Monitored at 500 nm)

solvent	τ_1 , ^a ps	A_1 , ^b %	τ_2 , ^c ps	A_2 , ^d %	τ_3 , ^e ns	A_3 , ^f %	dielectric constant
1,4-dioxane	7.2	0.24	178.11	15.34	4.7	84.40	2.22
acetone	0.26	0.01	54.69	0.99	4.81	98.99	21.0
acetonitrile	0.75	0.01	57.20	2.08	4.8	97.91	37.5
DMF	3.24	0.06	82.34	4.34	4.8	95.59	38.3
1-propanol	21.36	0.04	211.78	1.07	4.7	98.94	20.8
ethanol	4.61	0.06	147.85	10.91	4.6	89.03	24.3
methanol	3.83	0.03	73.70	1.45	4.8	98.52	32.6
water	1.36	0.03	71.58	2.27	4.6	97.69	80.0

^a ± 0.05 ps. ^b ± 0.21 %. ^c ± 1 ps. ^d 0.5%. ^e Lifetime obtained from TCSPC. ^f 2%.

the excitation pulse with the gate pulse gives an instrument response function with full width half-maximum (fwhm) of 300 fs. The fluorescence decay was fitted to Gaussian shape for the excitation pulse. The femtosecond fluorescent decay transients were analyzed by fixing the longer lifetime component obtained from TCSPC. All the experiments were carried out at 295 ± 1 K.

The time-resolved emission spectra of proflavine in different solvents was constructed by the technique elsewhere described.^{31,32} The femtosecond fluorescence decays of proflavine in different solvents was recorded over the entire emission spectrum from 460 to 600 at 10 nm intervals, and the decay at each wavelength was deconvoluted using the instrument response function with multiexponential model. A triexponential model was found to be adequate for all of the decays and a new set of decays was constructed using the fitted data. The constructed decays are normalized [$I(\lambda, t)$] so that the time-integrated intensity at each wavelength is equal to the steady state intensity at that wavelength.

Table 3. Time Constants (τ) and Relative Amplitudes (A) of Functions Used in Fitting the Femtosecond Emission Transients of Proflavine in Different Solvents (Excitation at 420 nm and Decay Monitored at 560 nm)

solvent	τ_1 , ^a ps	A_1 , ^b %	τ_2 , ^c ps	A_2 , ^d %	τ_3 , ^e ns	A_3 , ^f %	dielectric constant
1,4-dioxane	0.18	−0.01	196.55	14.91	4.7	85.11	2.22
acetone	0.86	−0.01	43.78	0.70	4.8	99.30	21
acetonitrile	0.33	−0.01	55.51	1.50	4.8	98.50	37.5
DMF	0.13	−0.01	91.65	2.82	4.8	97.18	38.3
1-propanol	77.99	−2.31	169.22	8.0	4.42	94.26	20.8
ethanol	7.72	−0.07	146.02	5.02	4.7	95.06	24.3
methanol	0.96	−0.01	81.77	1.13	4.7	98.86	32.6
water	0.16	−0.01	71.63	1.88	4.6	98.12	80

^a ± 0.1 ps. ^b ± 0.21 %. ^c ± 2 ps. ^d 0.5%. ^e lifetime obtained from TCSPC. ^f 2%.

Considering $F(\lambda)$ be the steady state emission spectrum, a set of $H(\lambda)$ values were calculated using the following equation

$$H(\lambda) = \frac{F(\lambda)}{\sum \alpha_i(\lambda) \tau_i(\lambda)}$$

where $\alpha_i(\lambda)$ and $\tau_i(\lambda)$ are the pre-exponential factor and decay time constants respectively at that wavelength. The intensity decay functions are then given by

$$I'(\lambda, t) = H(\lambda) I(\lambda, t)$$

The values of $I'(\lambda, t)$ are used to calculate the intensity at any wavelength and time, and thus the time-resolved emission spectra (TRES) are obtained. The emission maximum at different time was obtained by nonlinear least-squares fitting the TRES data to the log-normal line shape function as described by Maroncelli et al.³² Time-resolved area normalized emission

spectra (TRANES) were constructed by normalizing the area of each TRES spectrum such that the area of the spectrum at time t is equal to the area of the spectrum at the shortest time " t ". Area normalized spectra were performed using the Peakfit V4.12 software.

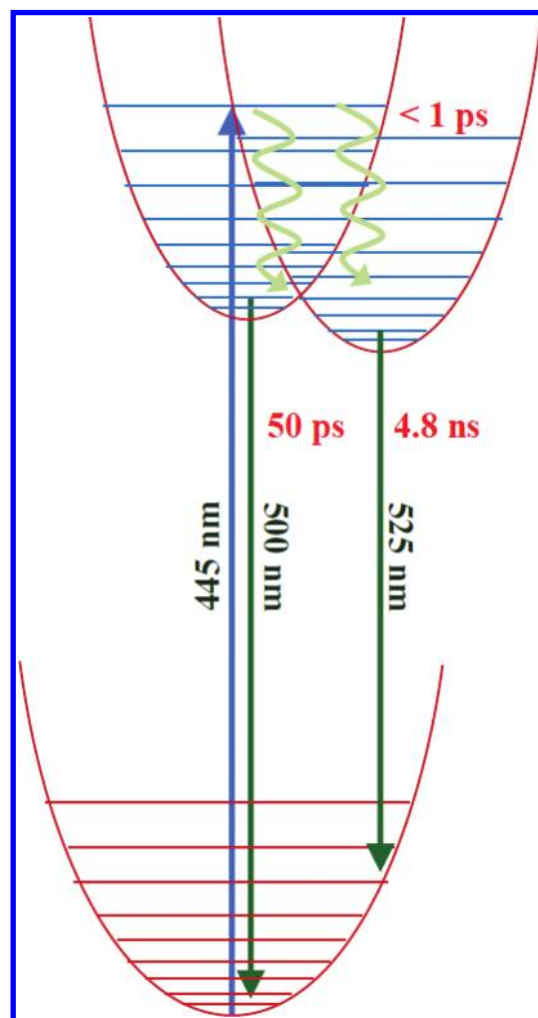
2.2. Computational Details. The electronic structure in the ground state S_0 of proflavine is investigated by Hartree–Fock (HF) computations using the 6-311++G** basis set. The two low-lying excited states S_1 and S_2 are studied by configuration interaction (CI) involving singly excited configurations at the 6-311++G** level.³³ The configuration interaction singles (CIS) study invoked all the excited configurations generated by single electron excitation from 20 highest occupied molecular orbitals (HOMOs) to 20 lowest virtual MOs. We have examined the molecular geometries in the ground and the excited states by complete structural optimization using the GAUSSIAN 03 software.³⁴ The computations are performed in the gas phase as well as in acetonitrile solvent. The solvent effect is taken into account using the COSMO model incorporated in the GAUSSIAN 03 software. Although it is well-known that the molecular geometries predicted at the above levels of calculations are reliable,³⁵ the excitation energies computed by the CIS study are invariably high on account of inadequate electron correlation. Hence we performed single-point density functional theory (DFT) calculations invoking B3LYP,^{33,36} B3P86,^{37,38} and LSDA^{39,40} functionals at the 6-311++G** level. The energies of the excited states are computed by time dependent DFT (TDDFT) calculations using the above functionals, invoking the same excited configurations that are included in the CIS study. The excitation energy is computed with reference to the ground state energy at the corresponding computational level. The TDDFT approach has been found to give remarkably good results for the low-lying vertical excitations.⁴¹

Although DFT study provides reliable predictions in a variety of systems, the TDDFT structural optimization on the excited states is computationally very time-consuming as the derivatives of energy are evaluated numerically, and hence we studied the excited state geometries by the CIS study.

3. RESULTS AND DISCUSSION

3.1. Steady State Absorption and Emission Spectral Studies. UV–visible absorption and emission spectra of proflavine obtained in various solvents are shown in Figure 1. The absorption spectra of the dye in the visible region in different solvents show a broad band with the maximum observed in the range 412 to 460 nm depending upon the solvent used. The photophysical characteristics of the dye in different solvents are given in Table 1. An increase in the polarity of the solvent leads to a blue shift in the absorption maximum, which is characteristic of charge transfer transition. In general, hydrogen bonding interaction, polarity of the solvent and specific solvent–solute interaction play a crucial role on the shift in absorption and emission spectral maximum of the dye.⁴² In the case of proflavine the shift in the absorption and emission spectral maximum could be correlated with the polarity and hydrogen bonding ability of the solvents. The absorption spectral maximum of proflavine in aqueous solution is observed at higher energy as compared to that in other polar protic and aprotic solvents. In the case of the dye dissolved in DMF, the absorption spectrum shows a blue shift as compared to that of the dye in aqueous solution even though polarity and hydrogen bonding ability of DMF is lower. In this case, specific

Scheme 1



solute–solvent interaction between the dye and DMF is the likely cause for the change in the spectral characteristics. The absorption and emission spectral shift of proflavine in alcoholic solvents show a linear behavior with dielectric constant of the solvent, whereas in the case of polar aprotic solvents the behavior is different as seen in Table 1, an observation similar to that reported earlier.^{43,44}

Fluorescence quantum yields for proflavine in different solvents are given in Table 1. The fluorescence quantum yield of the dye decreases with the increase in the polarity of the solvents used. The quantum yield of the dye in alcoholic solvents shows a linear response with the dielectric constant of the solvents. However, the fluorescence quantum yield of the dye in 1-propanol shows a higher fluorescence quantum yield as compared to those in ethanol and methanol. In the case of the dye in polar aprotic solvents THF and DMF, the fluorescence quantum yields are higher indicating specific solute solvent complex formation between the dye and the solvent molecule in the excited state.

3.2. Fluorescence Lifetime Studies. The fluorescence lifetime of proflavine in different solvents is determined on exciting the dye at 420 nm laser with the fluorescence decay monitored at the blue and red edges of the emission spectrum, and a typical decay profile is given in Figure 2. The fluorescence decay is fitted adequately using a single exponential function with the χ^2 value

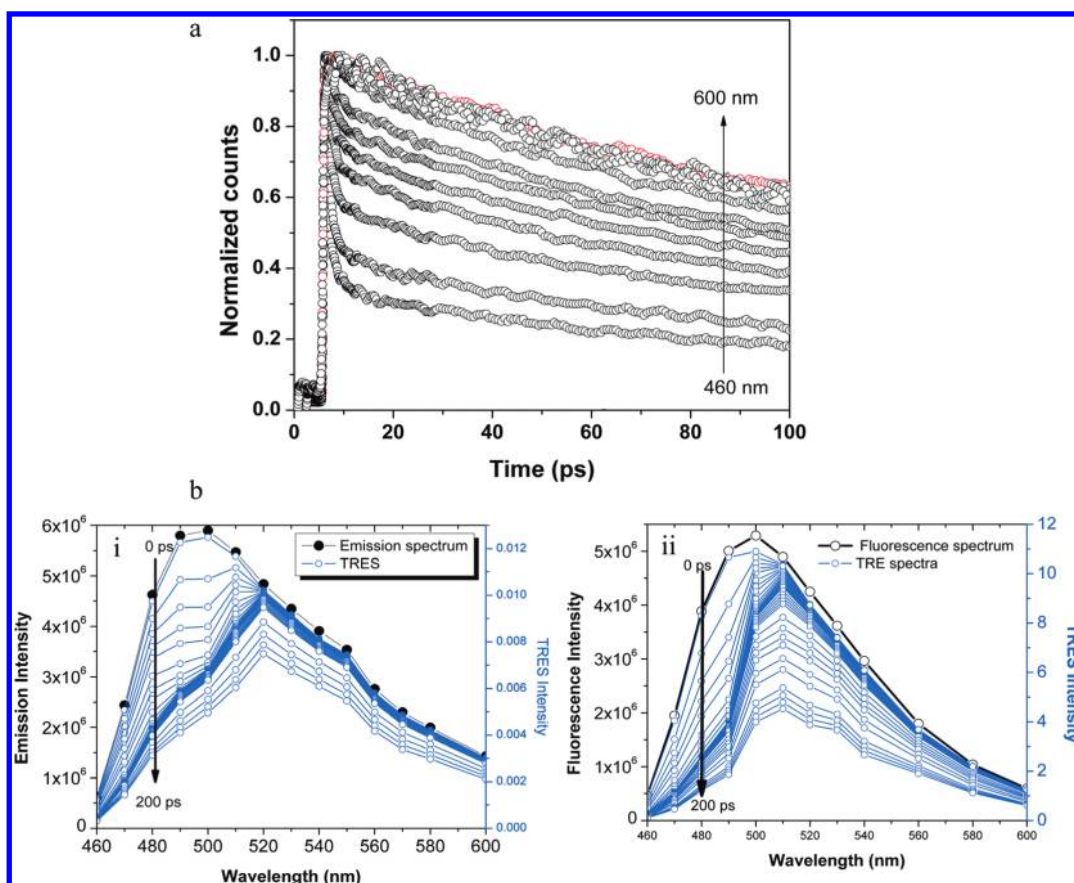


Figure 4. (a) Femtosecond fluorescence decay of proflavine in aqueous solution (excitation at 420 nm and decay monitored from 460 to 600 nm) and (b) time-resolved emission spectra of proflavine in (i) acetonitrile and (ii) acetone.

in the range 0.99–1.20. The fluorescence lifetime of proflavine does not vary with solvent polarity, whereas the Stokes shift and fluorescence quantum yield of the dye vary with solvent polarity as shown in Table 1. The observed invariance of the fluorescence lifetime in different solvents suggests that the excited proflavine relaxes through different emitting states in the homogeneous medium with one of the states presumably not affected by the solvent polarity. The plausible explanation is that (i) dipole moment of the dye in excited state is almost similar to that in the ground state or (ii) one of the states is preferentially affected by the solvent polarity which may have a shorter lifetime which is not observed in TCSPC setup with a time resolution of 50 ps. To confirm whether multiple emitting states are involved in the emission process, we have carried out fluorescence lifetime studies of proflavine in the femtosecond time domain in the solvents used, using femtosecond up-conversion technique. Investigation of the excited state dynamics of proflavine in femtosecond time domain in homogeneous media provides useful information on the excited state dynamics of the dye.

3.3. Femtosecond Dynamics of the Excited State Processes. Femtosecond fluorescence decay of proflavine observed upon 420 nm laser excitation in homogeneous solution in the 500 ps time window is shown in Figure 3. The femtosecond fluorescence decay of the dye is recorded with the concentration of the dye in the range 10^{-6} M to 10^{-5} M; in that concentration only the monocationic form of the dye is present in solution. It may also be noted that varying the pump energy (from ~ 0.1 to 0.4 nJ), does not change the decay constant.

The fluorescence decay of proflavine in homogeneous solution with femtosecond resolution is recorded at two wavelengths blue end (490 nm) and red end (600 nm) of the emission spectrum of proflavine and the fitted values of the decay profiles are given in Tables 2 and 3. Proflavine shows tri-exponential emission decay behavior in all the solvents used. Ultrafast decaying component (τ_1) of the dye varies when the decay is monitored at these two wavelengths. At the same time, decay time (τ_1) shows a rise time (pre-exponential term is negative) when the decay is monitored at the red part of the emission spectrum. The ultrafast time constant (τ_1) also varies with solvent polarity. Such behavior is an indication that the fluorescence originates from a different evolving excited state. As seen in Tables 2 and 3, proflavine shows an increase in the decay time (τ_1) with decreasing solvent polarity (methanol < ethanol < 1-propanol) that is attributed to the change in the characteristic solvation time of the excited state in these solvents. The solvation time measured for the excited state of coumarin 153 is 5 ps in methanol, 26 ps in 1-propanol, 0.26 ps in acetonitrile, and 0.58 ps in acetone.⁴⁵ On the basis of the above observations, we conclude that the main contribution of the ultrafast fluorescence decay is attributable to the solvation dynamics and relaxation pathway. In the case of the dye dissolved in aprotic solvents THF, ACN, acetone, and DMF, the observed ultrafast decay times are similar to the decay times reported in literature.⁴⁶

The ultrafast decay component (τ_2) observed in the femtosecond time domain does not change with emission wavelength, indicating that the emitting component of the dye is different in

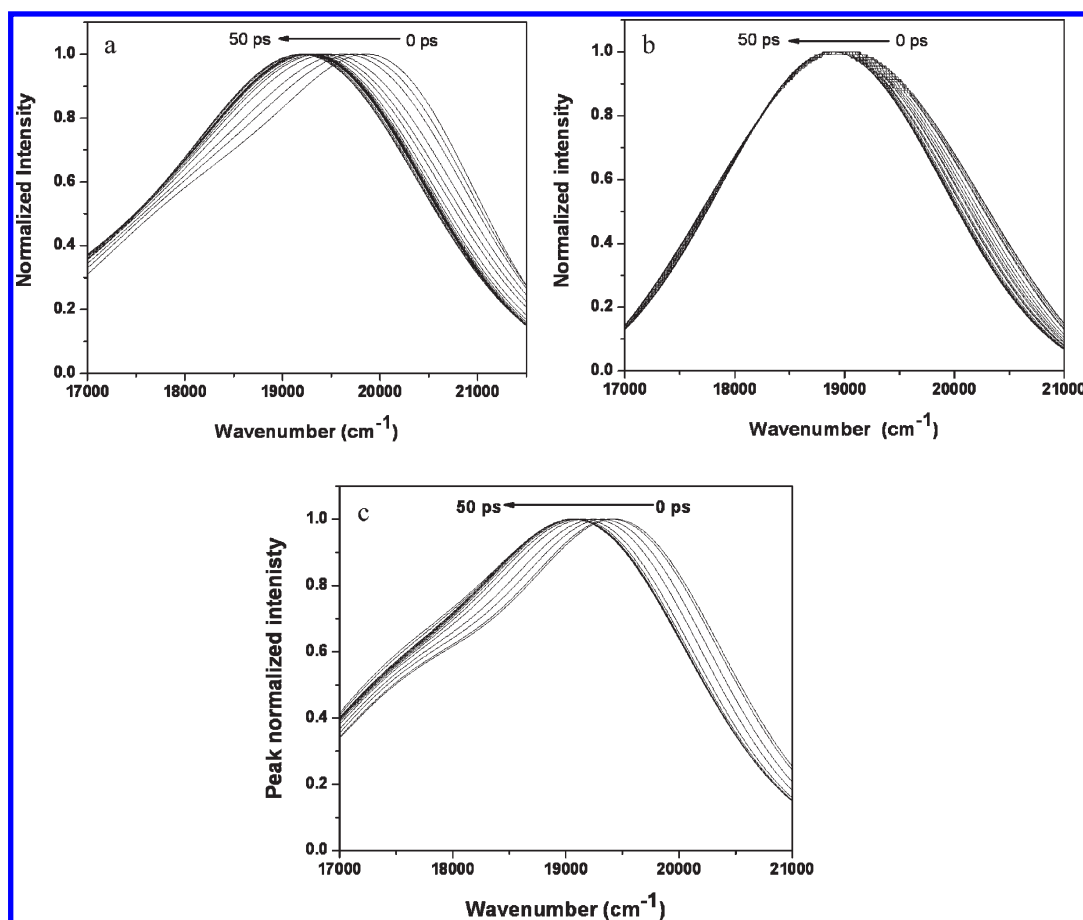


Figure 5. Time resolved emission spectra of proflavine in (a) acetone, (b) 1,4-dioxane, and (c) aqueous solution.

this case and not influenced by the solvation dynamics. The longer lifetime obtained from the TCSPC experiment (50 ns) is fixed during the femtosecond decay analysis and this longer lifetime is attributed to the emission from the relaxed excited state. The ultrafast decay component, τ_2 , observed in the range 50–215 ps depends up on the nature of the solvent. On the basis of the above observations, we conclude that the observed decay time around 50–215 ps depending on the polarity of the solvent is not due to solvation dynamics or vibration relaxation only. The observed decay times are presumably due to the emission from the close lying singlet excited states of proflavine in homogeneous media. It may be noted that the variation of the decay time τ_2 with solvent polarity suggests that the observed decay is primarily responsible for the variation in Stokes shift and fluorescence quantum yields of the dye with solvent polarity. The dye in polar protic solvents (Table 1) shows a more linear behavior for the ultrafast decay times τ_1 and τ_2 that correlates well with change in the fluorescence quantum yield of the dye with varying solvent polarity. The fluorescence decay monitored at the red edge of the emission spectrum also shows tri-exponential behavior with decay times of <1 ps, 70 ps, and 4.5 ns in different solvents. The relative contribution of $\tau_1 < 1$ ps shows a negative value for the amplitude which is attributed to the solvent relaxation or formation of relaxed state from the higher excited state.

In all the solvents, on excitation of proflavine, the Franck–Condon state (1B_2 state) is populated. The time constant, τ_1 , reflects the decay of the 1B_2 state accompanied with the solvation dynamics and population of 1A_1 state. The dipole moment of the

ground state is estimated to be 2.44 D, and those of the excited states 1B_2 and 1A_1 are estimated to be 4.13 and 3.17 D, respectively, by the quantum chemical methods. The change in dipole moment between the ground and 1B_2 excited state is large as compared to that for 1A_1 excited state. Due to the large dipole moment of the 1B_2 excited state, the interaction with the solvents is stronger. Relaxation of the Franck–Condon state (1B_2) involves both solvation and population transfer to the 1A_1 excited state. In the relaxation of 1B_2 state, the solvation and population transfer are coupled. There is no population transfer from the relaxed 1B_2 excited state to the 1A_1 excited state, and τ_2 reflects the lifetime of the relaxed 1B_2 excited state. The temporal resolution of the solvation dynamics and dynamics of the formation of 1A_1 excited state is not possible due to the coupled nature of the excited state processes. Details on the excited state dynamics of proflavine in homogeneous solution are given in Scheme 1. To further confirm the presence of two close lying emitting states in homogeneous environment, the time-resolved emission spectral studies of proflavine in various solvents of different polarity were carried out in femtosecond time domain using up-conversion technique.

3.3.i. Time Resolved Emission Spectral (TRES) Studies. The femtosecond fluorescence decay of proflavine monitored at different wavelengths from 460 to 600 nm is shown in Figure 4. Time resolved emission spectra (TRES) of the dye in different solvents are constructed following the method described earlier,³¹ and the results are presented in Figure 4i. TRES analysis shows that the spectral bandwidth and intensity profile of the dye

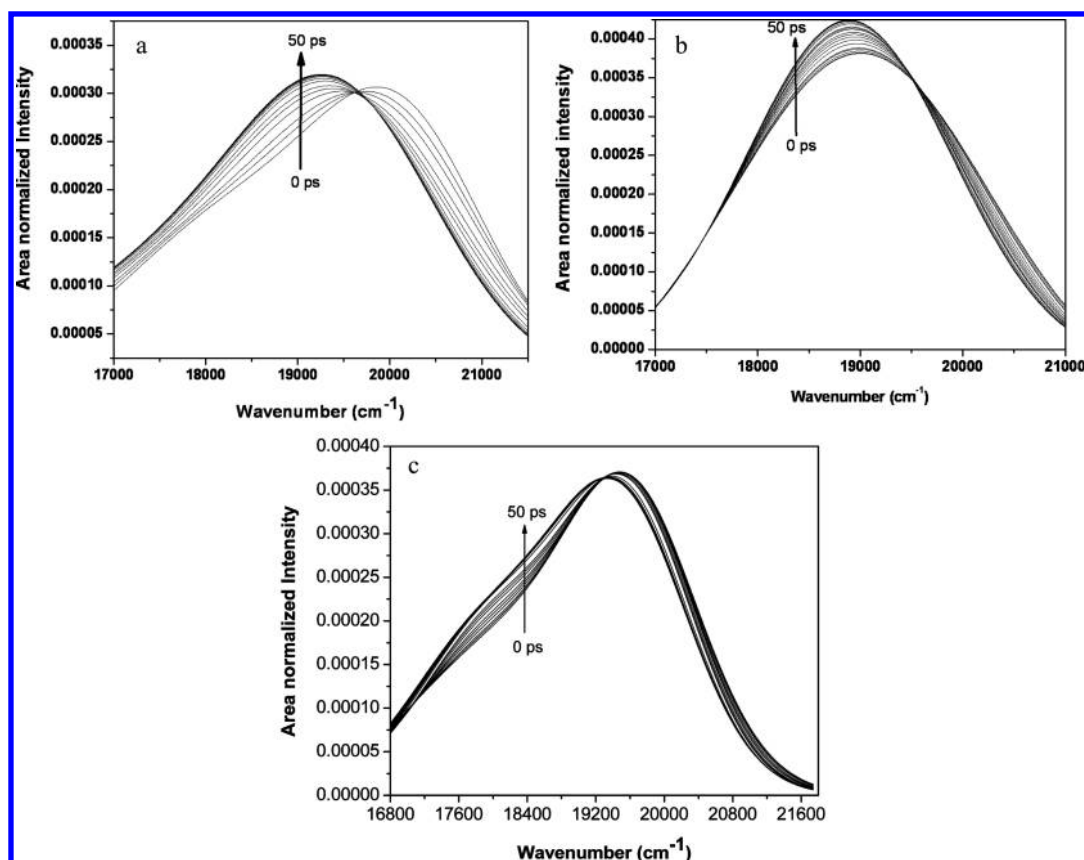


Figure 6. Time resolved area normalized emission spectra of proflavine in (a) acetone, (b) 1,4-dioxane, and (c) aqueous solution.

in different solvents vary with increasing time. At the same time, emission maxima are shifted from 490 to 520 nm. This observed decrease in the bandwidth with increasing time indicates that more than one emitting state is involved in the emission process. In addition to this, the reconstructed femtosecond time-resolved emission spectra of proflavine in acetonitrile at selected times are given in Figure 4ii. After the excitation, the maximum intensity is observed at 490 nm, which decays rapidly and the emission maximum shifts to 520 nm within ~ 1 ps. In the case of the dye dissolved in acetone, the emission maximum is shifted to 520 nm within ~ 6 ps. This observed result suggests that the emission originates from the excited state other than that produced on light absorption. TRES constructed for the dye in different solvents are given in Figure 5. The results obtained for all the solvents show red shift in the emission maximum with increasing delay time, which is presumably due to either one of the following factors involved in the photophysical process (i) solvation dynamics of the dye in the excited state or (ii) presence of two different species in the excited state or (iii) ground state heterogeneity.

3.3.ii. Time Resolved Area Normalized Emission Spectral (TRANES) Studies. To further confirm the presence of the close lying emitting states in the homogeneous solution, we have constructed the time-resolved area normalized emission spectra (TRANES) from the TRES obtained for the dye in various solvents. The time-resolved area normalized emission spectra are constructed by normalizing the area of each spectrum in TRES such that the area of the spectrum at time (t) is equal to the area of the spectrum at $t = 0$. The TRANES of the dye in various

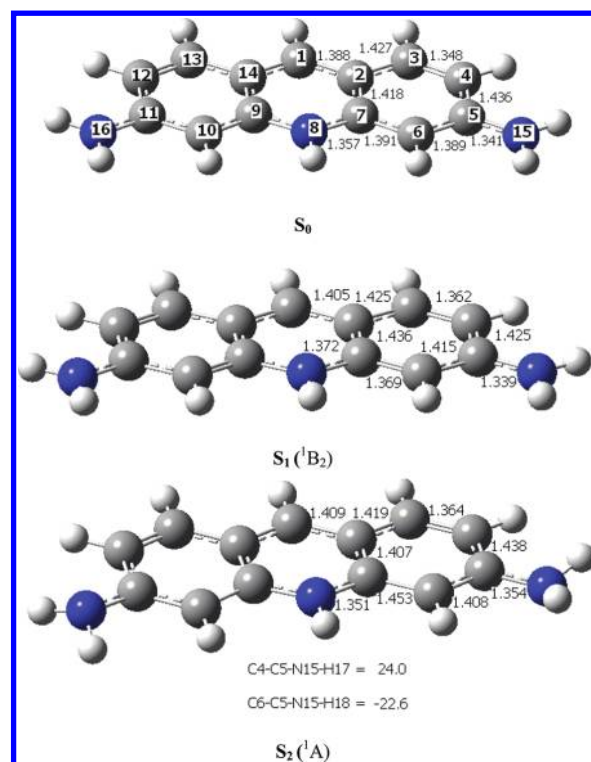


Figure 7. HF/6-311++G** optimized geometry of S0 and CIS/6-311++G** optimized geometries of S₁ (¹B₂) and S₂ (¹A₁). Bond lengths in angstroms and dihedral angles in degrees are shown.

Table 4. Adiabatic Excitation Energies of Proflavine in Acetonitrile Solvent

		excitation energies, nm (eV)				experimental emission maximum, nm (eV)
		single-point TD-DFT				
		CIS				
excited state	major excitation	CIS/6-311++G**	B3LYP/6-311++G**	LSDA/6-311++G**	B3P86/6-311++G **	
¹ B ₂ state	HOMO → LUMO (a2 → b1)	280.5 (4.42)	385.0 (3.22)	421.8 (2.94)	381.5 (3.25)	500 (2.48)
¹ A ₁ state	(HOMO−1) → LUMO (b → b)	255.1 (4.86)	396.1 (3.13)	447.7 (2.77)	392.4 (3.16)	512 (2.42)
shift in (nm)		25.4	10.9	25.9	10.9	12

solvents of different polarity are given in Figure 6, which shows an iso-emissive point. The observed iso-emissive point indicates two emitting species that are involved in the emission process. On the basis of the results obtained from femtosecond spectroscopy, the relaxation dynamics of proflavine in homogeneous solution is depicted in Scheme 1.

The solvatochromic probes such as coumarin have large change in dipole moment between ($\Delta\mu > 7$ D) the ground and excited state and shows time-dependent Stokes shift of less than 800 cm^{−1} for the solvent relaxation studies. For proflavine the change in dipole moment is low ($\Delta\mu = 1.69$ D), and for this low $\Delta\mu$ value, the time-dependent Stokes shift due to solvation dynamics is expected to be 100–200 cm^{−1}. But the proflavine exhibits a time-dependent Stokes shift of around 1200 cm^{−1}, which is presumably not due to the solvent relaxation alone. The unusual large Stokes shift indicates that the emission occurs from multiple excited states. TRANES is applicable for the systems where the large Stokes shift was observed at the ultrafast time scale. Rafiq et. al recently established the two state emission in ultrafast time scale (20 fs to 1.5 ps) in (4-nitrophenyl)-pyrrolidinemethanol using TRES and TRANES.⁴⁷ TRANES is indeed applicable to the time scale used in the present investigation. The TRES and TRANES results discussed are important to interpret the observed constant fluorescence lifetime (≈ 4.5 ns) of the dye in different solvents irrespective of the solvent polarity. The experimental results conform to the theoretical investigations (vide infra).

3.4. Geometries of the Excited States and Excitation Energies of Proflavine by Theoretical Study. The vertical excitation energy calculation at CIS/6-311++G** level shows that the lowest excited singlet S₁ state, ¹B₂ originates predominantly from the excitation of electron from the highest occupied MO (HOMO) of a₂ representation in the C_{2v} point group to the lowest unoccupied MO (LUMO) of b₁ representation. The second excited singlet state, ¹A₁ is formed by the excitation of electron from (HOMO−1) of the b₁ representation to the LUMO. Structural optimization of the S₁ state at the CIS/6-311++G** level leads to planar geometry which possesses C_{2v} point group as in the ground state. Thus the adiabatic S₁ of protonated proflavine is a ¹B₂ state. However, the second excited singlet state is found to relax to a nonplanar geometry possessing a C₂ axis of symmetry (C₂ point group). The amino groups of the proflavine deviate from the ring plane by about 25° in S₂, as predicted by the CIS/6-311++G** structural optimization. The adiabatic S₂ state is a ¹A₁ state. The ¹B₂ state is found to be long-axis polarized whereas the ¹A₁ state is short axis polarized.

The present study shows that the optimized geometries of the ground and excited states are very similar in the gas phase and in the acetonitrile dielectric medium. The optimized geometries in

Table 5. Dipole Moments (Debye) in the Optimized S₀, ¹B₂, and ¹A₁ States of Protonated Proflavine in the Gas Phase and Acetonitrile Solvent

state	method	dipole moment	
		gas phase	acetonitrile solvent
S ₀ (ground state)	HF/6-311++G**	1.68	2.44
¹ B ₂ state	CIS/6-311++G**	3.04	4.13
¹ A ₁ state	CIS/6-311++G**	2.72	3.17

acetonitrile medium are shown in Figure 7 along with selected bond lengths and dihedral angles.

Although the CIS results show that the ¹B₂ state is the lowest excited state, the single point TDDFT calculations performed on the CIS optimized geometries of the excited states ¹B₂ and ¹A₁ reveal that the nonplanar ¹A₁ state is the lowest energy emitting state. Dipole moments in the excited states of proflavine cation, computed using CI density, show a value of 3.17 D in the ¹A₁ excited state whereas it is 4.13 D in the ¹B₂ state in acetonitrile solvent (Table 4). It is seen that the dipole moment in the ¹A₁ excited state is closer to that in the ground state (2.44 D) as compared to that of the ¹B₂ state. A similar trend is also noticed in the gas-phase dipole moments of proflavine (Table 5). In the C₂ point group, the dipoles arising from the two NH₂ groups cancel each other as one of the amino groups is above the ring plane whereas the second amino group is below the ring plane. This may explain the small dipole moment of the ¹A₁ state. Because the observed lowest energy emission at 511 nm is independent of the polarity of the solvent, it may be inferred that it originates from the ¹A₁ state which is less polar than the ¹B₂ state. The TDDFT study using the B3LYP and LSDA functionals predicts that the ¹B₂ state emits at shorter wavelength, shifted by about 11 nm from that of the ¹A₁ state, which agrees closely with the observed shift of 12 nm. However, the calculations using the CIS method and the B3P86 functional show a corresponding shift of about 25 nm.

Table 5 shows that both the CIS and TDDFT methods overestimate the excitation energies. The LSDA40 results show the least deviation from the experimental frequencies as reported in the earlier studies.⁴¹ The deviations are 0.35 and 0.46 eV, respectively, for the states ¹A₁ and ¹B₂.

4. CONCLUSION

In this study, we presented detailed photophysics of proflavine in solvents with different solvent polarity. Proflavine shows solvent dependent spectral shifts in absorption and emission spectra whereas fluorescence lifetime is found to be independent

of solvent polarity. Quantum yields for fluorescence are determined in different solvents that vary with solvent polarity. Femtosecond dynamics of the emitting states indicates the decay time for excited state solvation. The femtosecond TRES and TRANES studies confirm the presence of two emitting states in homogeneous environment. The shorter lifetime component is responsible for change in Stokes shift and fluorescence quantum yields of the dye with solvent polarity. Detailed theoretical calculations using different formalisms including DFT calculations confirm the presence of two close lying excited states. The lowest energy excited state with the dipole moment similar to that of the ground state is interpreted to be responsible for the observed more or less constant fluorescence lifetime in different solvents of varying polarity. The reported investigation is of interest to further identify the excited states responsible for charge transfer process observed with suitable quenchers leading to hydrogen evolution.³

AUTHOR INFORMATION

Corresponding Author

*E-mail: pnatrajan@hotmail.com.

ACKNOWLEDGMENT

We acknowledge the financial support received from the Department of Science and Technology, Government of India, through the Raja Ramanna Fellowship to one of the authors P.N. The center is supported by DST-IRHPA programme. P.N. is the recipient of INSA-Senior Scientist award.

REFERENCES

- (1) Tsubomura, H.; Shimoura, Y.; Fujiwara, S. *J. Phys. Chem.* **1979**, *83*, 2103–2106.
- (2) Neumannspallart, M.; Kalyanasundaram, K. *J. Phys. Chem.* **1982**, *86*, 2681–2690.
- (3) Kalyanasundaram, K.; Dung, D. *J. Phys. Chem.* **1980**, *84*, 2551–2556.
- (4) Dejong, E. S.; Chang, C.; Gilson, M. K.; Marino, J. P. *Biochemistry* **2003**, *42*, 8035–8046.
- (5) Horowitz, E. D.; Hud, N. V. *J. Am. Chem. Soc.* **2006**, *128*, 15380–15381.
- (6) Li, S.; Cooper, V. R.; Thonhauser, T.; Lundowist, B. T.; Langreth, D. C. *J. Phys. Chem. B* **2009**, *113*, 11166–11172.
- (7) Pilani, M. P.; Gratzel, M. *J. Phys. Chem.* **1980**, *84*, 2402–2406.
- (8) Strauss, G.; Broyde, S. B.; Kurucsev, T. *J. Phys. Chem.* **1971**, *75*, 2727–2733.
- (9) Ananthanarayanan, K.; Natarajan, P. *Microporous Mesoporous Mater.* **2009**, *124*, 179–189.
- (10) Ananthanarayanan, K.; Selvaraju, C.; Natarajan, P. *Microporous Mesoporous Mater.* **2007**, *99*, 319–327.
- (11) Mertz, E. L. *J. Phys. Chem. A* **2005**, *109*, 44–56.
- (12) Ramstein, J.; Ehrenberg, M.; Rigler, R. *Biochemistry* **1980**, *19*, 3938–3948.
- (13) Strauses, G.; Broyde, S. B.; Kurucsev, T. *J. Phys. Chem.* **1971**, *75*, 2727–2733.
- (14) Qu, X.; Chaires, J. B. *J. Am. Chem. Soc.* **2001**, *123*, 1–7.
- (15) Ricci, C. G.; Netz, P. A. *J. Chem. Inf. Model* **2009**, *49*, 1925–1935.
- (16) Schwalb, N. K.; Temps, F. *J. Phys. Chem.* **2009**, *113*, 13113–13123.
- (17) Huang, Y.; Cheng, F.; Li, F.; Huang, H.; Wang, S.; Huang, W.; Gong, Q. *J. Phys. Chem. B* **2002**, *106*, 10041–10050.
- (18) Fujino, T.; Fujima, T.; Tahara, T. *J. Phys. Chem. B* **2005**, *109*, 15327–15331.
- (19) Kandori, H.; Tomioka, H.; Sasabe, H. *J. Phys. Chem. A* **2002**, *106*, 2091–2095.
- (20) Saha, S.; Samanta, A. *J. Phys. Chem. A* **2002**, *106*, 4763–4771.
- (21) Zgrablic, G.; Haacke, S.; Chergui, M. *J. Phys. Chem. B* **2009**, *113*, 4384–4393.
- (22) Miannay, F. A.; Gustavsson, T.; Banyasz, A.; Markovitsi, D. *J. Phys. Chem. A* **2010**, *114*, 3256–3263.
- (23) Gil, M.; Douhal, A. *J. Phys. Chem. A* **2008**, *112*, 8231–8237.
- (24) Senthil kumar, K.; Paul, P.; Selvaraj, C.; Natarajan, P. *J. Phys. Chem. C* **2010**, *114*, 7085–7094.
- (25) Samanta, A. *J. Phys. Chem. B* **2006**, *110*, 13704–13716.
- (26) Mintova, S.; De Waele, V.; Holzl, H.; Schmidhammer, V.; Mihailova, B.; Riedle, E.; Bein, J. *J. Phys. Chem. A* **2004**, *108*, 10640–10648.
- (27) Zhang, Y.; Wang, L.; Moss, R. A.; Platz, M. S. *J. Am. Chem. Soc.* **2009**, *131*, 16652–16653.
- (28) Zhang, H.; Raesh, C. S.; Dutta, P. K. *J. Phys. Chem. C* **2009**, *113*, 4623–4633.
- (29) Clarke, T. M.; Durrant, J. R. *Chem. Rev.* **2010**, *110*, 6736–6767.
- (30) Drexhage, K. H. *J. Res. Natl. Bur. Stand. A* **1976**, *80A*, 421.
- (31) Koti, A. S. R.; Krishna, M. M. G.; Periasamy, N. *J. Phys. Chem. A* **2001**, *105*, 1767–1771.
- (32) Lakowicz, J. R. *Principles of fluorescence spectroscopy*, 3rd ed.; Springer: Berlin, 2006.
- (33) Hornig, M. L.; Gardecki, J. A.; Papazyan, A.; Maroncelli, M. *J. Phys. Chem.* **1995**, *99*, 17311.
- (34) Foresman, J. B.; Head-Gordon, M.; Pople, J. A.; Frisch, M. J. *J. Phys. Chem.* **1992**, *96*, 135.
- (35) Frisch, M. J. et al. *Gaussian 03*, Revision B.05; Gaussian, Inc.: Wallingford, CT, 2004.
- (36) Foresman, J. B.; Frisch, A. *Exploring Chemistry with Electronic Structure Methods*; Gaussian, Inc.: Pittsburgh, PA, 1996.
- (37) Becke, A. D. *J. Chem. Phys.* **1993**, *98*, 5648.
- (38) Lee, C.; Yang, W.; Parr, R. G. *Phys. Rev. B* **1988**, *37*, 785.
- (39) Perdew, J. P. *Phys. Rev. B* **1986**, *33*, 8822.
- (40) Slater, J. C. *The Self-Consistent Field for Molecular and Solids; Quantum Theory of Molecular and Solids*; McGraw-Hill: New York, 1974; Vol. 4.
- (41) Vosko, S. H.; Wilk, L.; Nusair, M. *Can. J. Phys.* **1980**, *58*, 1200.
- (42) Hsu, C. P.; Hirata, S.; Head-Gordon, M. *J. Phys. Chem. A* **2001**, *105*, 451.
- (43) Mertz, E. L.; Tikhomirov, V. A.; Krishtalik, L. I. *J. Phys. Chem. A* **1997**, *101*, 3433.
- (44) Jarzeba, W.; Walker, G. C.; Johnson, A. E.; Kahlow, M. A.; Barbara, P. F. *J. Phys. Chem.* **1988**, *92*, 7039.
- (45) Maroncelli, M.; Fleming, G. R. *J. Chem. Phys.* **1987**, *86*, 6221.
- (46) Glasbeek, M.; Zhang, H. *Chem. Rev.* **2004**, *104*, 1929.
- (47) Kahlow, M. A.; Jarzelo, W.; Kang, J. T.; Barbara, P. F. *J. Phys. Chem.* **1989**, *90*, 151.
- (48) Rafiq, S.; Yadav, R.; Sen, P. *J. Phys. Chem. A* **2011**, *115*, 8335.